Kink Stochastics

Kinks are examples of coherent structures: clearly identifiable localized features in a noisy, spatially extended system that can be followed as they move about under the influence of fluctuations. Numerical convergence of thermodynamic properties lets us explore kinks' stochastic dynamics.

Scientists in many fields face a similar challenge: to understand a large system, driven by many noisy and nonlinear influences, and containing persistent identifiable structures. They're meeting the challenge with a two-pronged approach. First, using the most powerful computers available, scientists perform numerical simulations of the full model on the largest domain and with the highest spatial resolution possible, for as long a time as possible. Second, they've developed theoretical methods that efficiently identify the structures of interest and predict their number, structure, dynamics, and interactions.

Identifying Kinks

The following stochastic partial differential equation (SPDE) describes the evolution of a random field in one space dimension:

$$\frac{\partial}{\partial t}\Phi_t(x) - \frac{\partial^2}{\partial x^2}\Phi_t(x) =$$
$$\Phi_t(x) - \Phi_t^3(x) + (2KT)^{1/2}\xi_t(x). \quad (1)$$

At time t, the field is a continuous function of x denoted Φ_t; at time t and position x, it's a real-valued random variable denoted $\Phi_t(x)$. The last term in Equation 1 is space-time white noise:

$$\langle \xi_t(x)\xi_{t'}(x') \rangle = \delta(x - x')\delta(t - t'). \quad (2)$$

(Angled brackets indicate mean over realizations.) In the amplitude $(2KT)^{1/2}$, T is temperature and K is Boltzmann's constant. We use the notation $\beta = (KT)^{-1}$.

At a fixed time in one realization of the SPDE, the field is a continuous function of x called a *configuration*. A typical configuration consists of long regions in which the field is close to ±1 and separated by boundaries (see Figure 1). A boundary with a region close to –1 to the left and a region close to +1 to the right is a *kink*; the opposite case is an *antikink*. At low temperatures, these kinks are good examples of coherent structures.

We can identify and follow kinks and antikinks as they move about due to constant fluctuations along the spatial domain. Kinks and antikinks alternate along every configuration. New kinks and

GRANT LYTHE

University of Leeds

SALMAN HABIB

Los Alamos National Laboratory

antikinks are created and existing ones destroyed, always in pairs. We'll be interested in large domains and periodic boundary conditions to obtain a large number of kinks and eliminate end effects.

The SPDE (see Equation 1) is the overdamped limit of the ϕ^4 model with space-time white noise, which mathematicians, scientists, and engineers have studied extensively as a model with nonlinear coherent structures.[1] Here, we restrict ourselves to one space dimension, in which these structures are known as kinks. If we define the potential, $V(\phi) = (-1/2\phi^2 + 1/4\phi^4)$, and the energy functional,

$$\mathcal{E}[f] = \int \left(V(f(x)) + \frac{1}{2}\left(\frac{\partial}{\partial x}f(x)\right)^2 \right) dx, \qquad (3)$$

the SPDE (Equation 1) is

$$d\Phi_t(x) = -\frac{\delta\mathcal{E}(\Phi_t)}{\delta\Phi_t(x)}dt + (2KT)^{1/2}d\mathbf{B}_t(x), \qquad (4)$$

where $\langle d\mathbf{B}_t(x)d\mathbf{B}_{t'}(x')\rangle = \delta(x-x')\delta(t-t')dt$. The *single-kink solution* is the function $\phi(y) = \tanh(y/\sqrt{2})$, which is the solution of the ordinary differential equation $V'(\phi(y)) = \phi''(y)$ with $\lim_{x\to-\infty}\phi(x) = -1$ and $\lim_{x\to\infty}\phi(x) = 1$. The single-kink solution gives a kink's shape and characteristic width. Moreover, the quantity $\mathcal{E}[\phi] = E_k$ is the kink's mass.

Kink Dynamics and the Steady State

Isolated kinks and antikinks follow Brownian paths. When a kink and an antikink meet, they annihilate. However, the noise also produces new kink–antikink pairs. Such nucleation events occur at random times and positions with rate[2]

$$\Gamma \propto \exp(-2\beta E_k). \qquad (5)$$

If we solve Equation 1, starting from $\Phi_t(x) = 1$ for all x, for example, we find a well-defined steady-state density of kinks and antikinks, ρ, after a relaxation time proportional to Γ^{-1}.

Once it's in the steady state, we can think of the system evolving according to Equation 1 as sampling from the steady-state density in the space of continuous functions.[3] Consequently, we can calculate many late-time properties of the SPDE's solutions analytically. For example, the correlation function,

$$c(x) = \lim_{t\to\infty}\left\langle \Phi_t(y)\Phi_t(y+x) \right\rangle, \qquad (6)$$

is independent of y. As $x \to \infty$,

t = 2,300
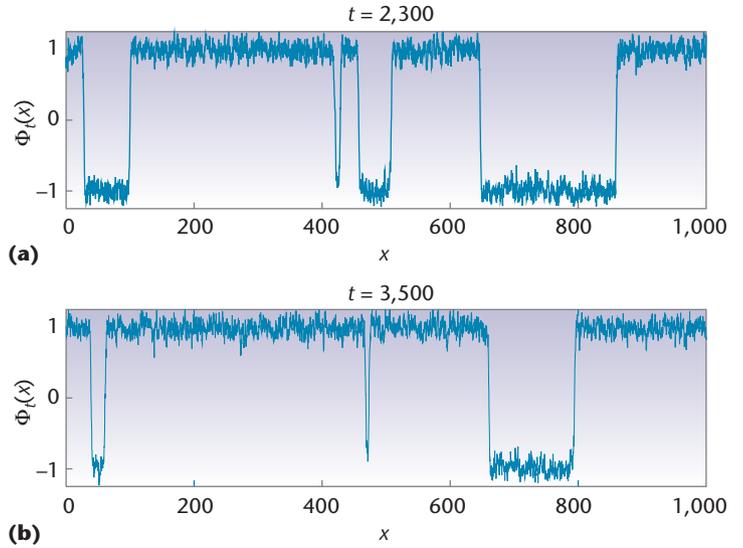
(a)

t = 3,500

(b)

Figure 1. Two configurations from one numerical realization ($\beta = 40$). Kinks and antikinks alternate along every configuration. New kinks are created (*nucleation*) and existing ones destroyed (*annihilation* on collision), always in pairs.

$$c(x) \to \exp(-x/\lambda). \qquad (7)$$

The correlation length λ is given by

$$\lambda = (\beta(\varepsilon_1 - \varepsilon_0))^{-1}, \qquad (8)$$

where ε_0 and ε_1 are the two smallest eigenvalues of the equation

$$\left(-\frac{1}{2\beta^2}\frac{\partial^2}{\partial u^2} - \frac{1}{2}u^2 + \frac{1}{4}u^4\right)\psi_n(u) = \varepsilon_n\psi_n(u). \qquad (9)$$

The fact that kink–antikink pairs are nucleated at random times and positions isn't sufficient to produce a random kink distribution because the colliding kink and antikink annihilation generally produces a steady state in which the kinks are less likely to be closer to each other than they would be under a random distribution.[4] However, the length scale λ^{-1} that determines the mean separation between kinks is proportional to $\exp(E_k\beta)$; at sufficiently low temperatures, it's hugely larger than the typical separation of a kink–antikink pair at the instant of nucleation.[5–7] Consequently, the kink and antikink distribution is very close to a random distribution, and the density of kinks and antikinks is related to λ by
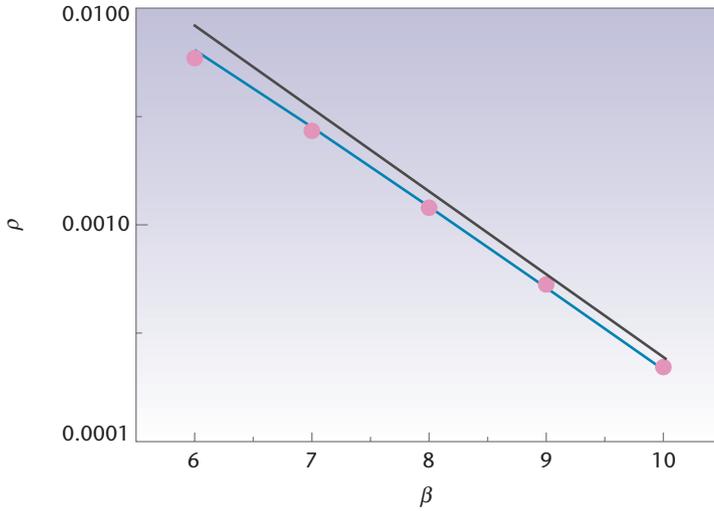
$$\rho = \frac{1}{2}\frac{1}{\lambda}. \qquad (10)$$

Figure 2. Kink density versus inverse temperature (log scale). The dots are densities measured from numerical solutions of the stochastic partial differential equation (SPDE; Equation 1). The blue line is Equation 10, which gives the correlation length λ from Equation 8. The gray line uses the WKB approximation to the eigenvalues of Equation 9. As $T \to 0$, the number of kinks per unit length is proportional to $\exp(-E_k \beta)$. To precisely compare numerical and exact results at finite temperature, it's important to use the exact correlation length and not the WKB approximation.

For $\beta \lesssim 10$, we can undertake numerical solutions on domains large enough to contain thousands of kinks, and thus obtain accurate estimates of the mean number of kinks per unit length in the steady state. Figure 2 compares the kink density as measured from numerical solutions with the prediction in Equation 10, where Equation 8 gives λ. Equation 9's solution gives us the eigenvalues ε_0 and ε_1 on the blue line. The gray line uses the Wentzel-Kramers-Brillouin (WKB) approximation[8] to those eigenvalues, which improves as the temperature T decreases (as β increases). We use a log scale, so the difference between the two amounts to tens of percent for the values of β displayed. The density as measured from careful numerical solutions of the SPDE is sufficiently accurate to resolve the difference between the exact value of λ and the WKB approximation to it.

Numerics

We use the method of finite differences, which generates a numerical solution on a grid of points separated by Δx.[3] This converts the SPDE into a system of coupled SDEs:

$$d\Phi_t(x) = (\Phi_t(x) - \Phi_t^3(x) + \tilde{\Delta}\,\Phi_t(x))dt + (2KT)^{1/2}d\mathbf{B}_t(x), \qquad (11)$$

where

$$\tilde{\Delta}\Phi_t(x) = (\Phi_t(x + \Delta x) + \Phi_t(x - \Delta x) - 2\Phi_t(x))\Delta x^{-2}. \qquad (12)$$

We can think of the system dynamics discretized in space as a string of coupled overdamped oscillators subject to three competing influences: a double-well onsite potential, coupling to neighboring sites, and random fluctuations. Figure 3 shows an example of a part of a configuration (values of $\Phi_t(x)$ at one time and a range of x values).

To solve the system discretized in space, we also discretize in time and generate realizations, each consisting of a long series of configurations. Each discretized configuration consists of $\Phi_t(x)$ at a large number (typically 10^6) of x values. The notation in Equation 11 expresses in a natural way the algorithm used to solve the SPDE numerically. In the Euler time-stepping algorithm, the change between time t and time $t + \Delta t$ in the value of the field at grid point x, $\Phi_t(x)$, is

$$\Phi_{t+\Delta t}(x) - \Phi_t(x) = (\Phi_t(x) - \Phi_t^3(x) + \tilde{\Delta}\Phi_t(x))\Delta t + (2KT)^{1/2}\Delta\mathbf{B}_t(x), \qquad (12)$$

where $\Delta\mathbf{B}_t(x)$ is a Gaussian random variable for each x and t with mean zero and

$$\langle\Delta\mathbf{B}_t\Delta\mathbf{B}_{t'}(x')\rangle = \begin{cases} \dfrac{\Delta t}{\Delta x} & x = x' \text{ and } t = t' \\ 0 & \text{otherwise} \end{cases}. \qquad (13)$$

We can perform the time stepping itself using the second-order stochastic Runge-Kutta (Heun) method[9] because the SPDE discretized in space is a set of coupled equations with additive noise. In the discretized Laplacian, the grid spacing Δx appears as $\Delta t\Delta x^{-2}$. The scaling $\Delta t \propto \Delta x^2$ is thus necessary in parabolic PDEs.[10] Explorations to date suggest the same is true for their stochastic counterparts.[11] That is, when we compare the numerical results obtained at different values of Δx, we must scale Δt proportional to Δx^2.

In addition to questions of the numerical scheme's convergence, we're often interested in the low temperature limit ($\beta \gg 1$). This limit is convenient for analytical approximations and for unambiguous identification of coherent structures, but requires large amounts of computer time. Two reasons for the increase in computer time with decreasing temperature are

- The system's timescales typically increase exponentially as temperature decreases, so we must

perform runs of increasing duration to attain the steady state from an arbitrary initial condition.

- The density of coherent structures also decreases with decreasing temperature, so we need ever-larger systems to obtain good statistics.

In the 1980s, it was only possible to perform numerics at low resolution ($\Delta x \simeq 1.0$) and high temperatures ($\beta \leq 5$), yielding steady-state densities that differed from the theoretical values by tens of percent. Some studies resorted to ad hoc "effective temperatures" to obtain better apparent agreement between numerical and theoretical steady-state properties, and some authors even suggested that the nucleation rate relation in Equation 5 was incorrect.[7] Fortunately, parallel machines available since the 1990s and 21st-century desktop computers can attain sufficient resolution to perform direct comparisons with transfer-integral predictions for the steady state and sufficiently low temperatures to unambiguously locate kinks and identify nucleation events.

Timescales

Because the SPDE (Equation 1) is solved directly, we can explore not only the steady state, but also the full dynamics. In particular, we can follow individual kinks' and antikinks' space-time trajectories.

How long do kinks live? Let's denote by τ a kink or antikink's mean lifetime in the steady state. The steady-state density of kinks is $\rho \propto \exp(-\beta E_k)$, and Equation 5 gives the rate of nucleation of new kink–antikink pairs. With the relationship $\rho = \Gamma\tau$, we can conclude that[5,6]

$$\tau \propto \exp(E_k\beta), \tag{13}$$

and confirm it by explicitly following kink trajectories.[7]

Markus Büttiker and Thomas Christen introduced an intuitive way to understand the mean lifetime scaling.[5] Consider the fate of a Brownian particle starting at $x = b$ in a domain with absorbing boundaries at $x = 0$ and $x = L$ (see Figure 4). The mean time to absorption is

$$\tau_L = \frac{bL}{2D}. \tag{14}$$

If we choose $L \propto \rho^{-1}$, we find $\tau \propto \rho^{-1}$.

Analysis of the following model provides further understanding of kink lifetimes. Kinks and antikinks are approximated by point particles that are nucleated in pairs at random times and posi-
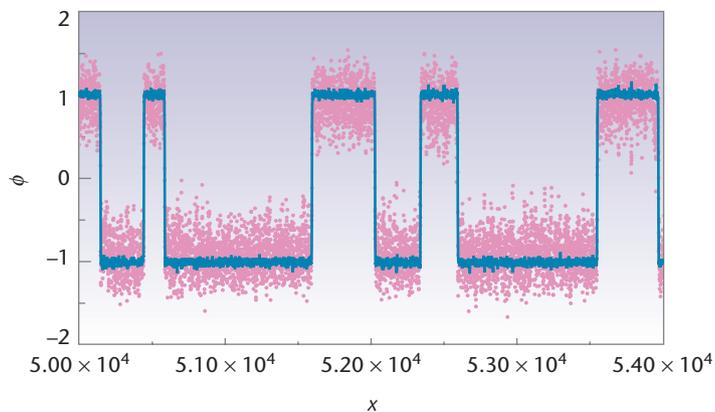
Figure 3. Part of a numerical configuration with $\beta = 8$. The dots are values at grid points, and the blue line is a smoothed interpolation. Kinks and antikinks alternate along the x direction.

Figure 4. Mean exit time. From the domain [0, L] of a Brownian particle, with diffusivity D and initial condition b, the mean exit time is $\tau_L = bL/2D$.

tions at rate Γ with separation b, have diffusivity D, and annihilate on collision. We can calculate particle density as a function of time exactly.[4] As $b(\Gamma/D)^{1/3} \to 0$, the steady-state density is given by

$$\rho = \left(\frac{b\Gamma}{2D}\right)^{1/2}. \tag{15}$$

The mean particle lifetime is then

$$\tau = \frac{\rho}{2\Gamma} = \left(\frac{b}{8D\Gamma}\right)^{1/2} = \frac{b}{4D\rho}. \tag{16}$$

In the opposite limit, when the mean distance between particles in the steady state is comparable to the separation of newly nucleated pairs, we find the scaling $\rho \propto \Gamma^{1/3}$.[4]

As we discussed earlier, the mean separation between kinks increases exponentially fast as $KT \to 0$. It's also vastly larger than the typical separation between the kink and antikink forming a newly nucleated pair, which is several times the kink width. The kink system is then in the regime described by Equation 15. On the other hand, the high-temperature limit isn't relevant because the very identification of kinks as well-defined structures is

problematic. The diffusivity of an isolated kink is given by[12]

$$D = \frac{E_k}{KT} + \mathcal{O}\left(\left(\frac{E_k}{KT}\right)^2\right). \qquad (17)$$

Although the existence of a short-range attraction between kinks and antikinks makes obtaining an independent estimate for b difficult, large-scale simulations are consistent with Equation 15.

To understand not only the mean but also the distribution of lifetimes, we classify each kink's history by whether it ends in an annihilation event with the antikink it was nucleated with (recombination) or with some other antikink. Recombination is far more likely because the distance between newly nucleated pairs is much smaller than the inverse of the steady-state density of kinks, so their Brownian paths are more likely to intersect.[5,7] Rarer nonrecombinant annihilation events leave behind a *survivor* kink (a kink whose partner is no longer alive) that has a long lifetime. We observe that these two effects cancel out almost exactly, so that *paired* kinks (those whose partners are still alive) and survivor kinks are present in similar numbers in the steady state.

A surprisingly good approximation for the probability density of the time between nucleation of a kink–antikink pair and annihilation of one or both is[7]

$$R(t) = N \exp\left(-\frac{b^2}{8Dt}\right) t^{-3/2} \exp(-18D\rho^2 t). \quad (18)$$

The approximations leading to Equation 18 ignore the short-range attraction between kinks and antikinks and assume that the probability per unit time that one member of a kink–antikink pair collides with another kink or antikink is a constant.

We can analyze the dynamics of a system containing many kinks and antikinks by analogy with a chemical rate equation. Because kinks and antikinks react in pairs, the standard chemical rate equation would read

$$\rho = 2\Gamma - k\rho^2 \qquad (19)$$

for some constant k. However, Equation 19 can't correctly describe the dynamics.[13] In fact, no closed polynomial rate equation can capture the qualitative aspects of the density's dynamics even for the simplified point-particle model. A promising alternative is to construct an effective theory for the two densities $n_p(t)$ (paired kinks) and $n_s(t)$ (survivor kinks).[7]

Although many aspects of the present state of knowledge are pleasing—such as clear intuitive understanding of time and length scales, precise comparison between theory and numerics, and control over convergence—important questions remain. What is the precise value of b, the separation between a kink and an antikink at nucleation? Can we construct and solve an effective macroscopic model that includes the kink–antikink attraction for separations of order b or less? Can we make a first-principles calculation for the nucleation rate Γ? How should we describe the ballistic dynamics of kinks and their collisions when the SPDE is second order in time?

The interaction of noise and nonlinearity in spatially extended systems remains a fertile ground for future research. Emergence of persistent coherent structures from localized fluctuations is a common phenomenon in sciences ranging from oceanographics to superconductivity. Researchers have used the 1D equation that is this article's focus as a general model for a chain of coupled double-well oscillators,[14] to model specific physical systems such as the polymer polyacetalene, charge-density-wave condensates, and Josephson-junction transmission lines.[1] From a theoretical viewpoint, the ϕ^4 SPDE is interesting because it lets us rigorously reduce the full spatiotemporal dynamics to an effective dynamics for the kinks, and because exact continuum results are available with which we can precisely compare numerical results, necessarily obtained in discrete space. **CiSE**

References

1. A.R. Bishop, J.A. Krumhansl, and J.R. Schrieffer, "Solitons in Condensed Matter: A Paradigm," *Physica D*, vol. 1, no. 1, 1980, pp. 1–44.

2. M. Büttiker and R. Landauer, "Nucleation Theory of Overdamped Soliton Motion," *Physical Rev. Letters*, vol. 43, no. 20, 1979, pp. 1453–1456.

3. G. Lythe and S. Habib, "Stochastic PDEs: Convergence to the Continuum?" *Computer Physics Comm.*, vol. 142, 2001, pp. 29–35.

4. S. Habib et al., "Diffusion-Limited Reaction in One Dimension: Paired and Unpaired Nucleation," *J. Chemical Physics*, vol. 115, no. 1, 2001, pp. 73–89.

5. M. Büttiker and T. Christen, "Nucleation of Weakly Driven Kinks," *Physical Rev. Letters*, vol. 75, no. 10, 1995, pp. 1895–1898.

6. M. Buttiker and T. Christen, "Diffusion Controlled Initial Recombination," *Physical Rev. E*, vol., 58, no. 2, 1998, pp. 1533–1542.

7. S. Habib and G. Lythe, "Dynamics of Kinks: Nucleation, Diffusion, and Annihilation," *Physical Rev. Letters*, vol. 84, no. 6, 2000, pp. 1070–1073.

8. D.J. Scalapino, M. Sears, and R.A. Ferrell, "Statistical Mechanics of One-Dimensional Ginzburg-Landau Fields," *Physical Rev. B*, vol. 6, no. 9, 1972, pp. 3409–3416.

9. P.E. Kloeden and E. Platen, *Numerical Solution of Stochastic Differential Equations*, Springer, 1992.

10. L. Lapidus and G.F. Pinder, *Numerical Solution of Partial Differential Equations in Science and Engineering*, Wiley, 1982.

11. G. Lythe and S. Habib, "Kinks in a Stochastic PDE," *Proc. International Union of Theoretical and Applied Mechanics Symp. Nonlinear Stochastic Dynamics*, N. Sri Namachchivaya and Y.K. Lin, eds., Kluwer, 2003, pp. 435–444.

12. D.J. Kaup, "Thermal Corrections to Overdamped Soliton Motion," *Physical Rev. B*, vol. 27, no. 11, 1983, pp. 6787–6795.

13. K. Kang and S. Redner, "Scaling Approach for the Kinetics of Recombination Processes," *Physical Rev. Letters*, vol. 52, no. 12, 1984, pp. 955–958.

14. S. Aubry, "United Approach to Interpretation of Displacive and Order-Disorder Systems. 1. Thermodynamical Aspect," *J. Chemical Physics*, vol. 62, 1975, pp. 3217–3227.

Grant Lythe is a permanent lecturer in applied mathematics at the University of Leeds. He is an editor of UK Nonlinear News. His research interests include stochastic ordinary and partial differential equations, diffusion-limited reaction and coherent structures, and numerical stochastics. Lythe has a PhD in applied mathematics from the University of Cambridge. He is a member of the Society for Industrial and Applied Mathematics. Contact him at grant@maths.leeds.ac.uk.

Salman Habib is a technical staff member at Los Alamos National Laboratory. His research interests include dynamics—nonlinear and stochastic—of classical and quantum field theories and applications in particle physics, condensed matter systems, atomic and quantum optics, accelerator physics, and cosmology. Habib has a PhD in physics from the University of Maryland, College Park. He is a member of the American Physical Society. Contact him at habib@lanl.gov.